# Selective Excitation of Tropical Atmospheric Waves in Wave–CISK: The Effect of Vertical Wind Shear

MINGHUA ZHANG AND MARVIN A. GELLER

*Institute for Terrestrial and Planetary Atmospheres, State University of New York at Stony Brook, Stony Brook, New York*

(Manuscript received 17 August 1992, in final form 24 May 1993)

ABSTRACT

The growth of waves and the generation of potential energy in wave–CISK require unstable waves to tilt with height oppositely to their direction of propagation. This makes the structures and instability properties of these waves very sensitive to the presence of vertical shear in the basic flow. Equatorial Kelvin and Rossby–gravity waves have opposite phase tilt with height to what they have in the stratosphere, and their growth is selectively favored by basic flows with westward vertical shear and eastward vertical shear, respectively. Similar calculations are also made for gravity waves and Rossby waves. It is shown that eastward vertical shear of the basic flow promotes CISK for westward propagating Rossby–gravity, Rossby, and gravity waves and suppresses CISK for eastward propagating Kelvin and gravity waves, while westward shear of the basic flow has the reverse effects.

## 1. Introduction

Since the theoretical development and the subsequent observational discovery of mixed Rossby–gravity waves and Kelvin waves in the tropical stratosphere (Matsuno 1966; Yanai and Maruyama 1966; Wallace and Kousky 1968), there have been many efforts to study potential sources of these waves in the troposphere. Spectral studies have shown that tropospheric variables in the tropics have a very broad range of frequencies (Wallace 1973). Although it is generally believed that the low-frequency 30–50-day oscillations discovered by Madden and Julian (1972) are eastward propagating Kelvin waves (Lau and Peng 1987; Swinbank et al. 1988), and that some of the 4–5-day peaks that are observed in many meteorological variables have been identified as westward propagating Rossby–gravity waves (Hendon and Liebmann 1991), studies of tropical waves in the troposphere are still quite uncertain as far as several basic questions are concerned.

First, what are the sources of tropical waves? Three possibilities have been proposed. One is the generation of tropical waves from lateral forcing at subtropical latitudes (Mak 1969). Numerical experiments by Hayashi and Golder (1978), in which midlatitude forcing was imposed and then removed, indicated, however, that lateral boundary forcing was not the primary driving force of tropical waves in these experiments. Nevertheless, many studies do suggest that midlatitude circulations have large impacts on tropical waves (Zangvil and Yanai 1980; Yanai and Lu 1983; Itoh and Ghil 1988). The second theory assumes tropical waves to be forced by variable tropical convective heating (Holton 1972; Salby and Garcia 1987). The third theory is that of wave–CISK. Here, it is considered that waves are self-maintained by the latent heat released in convection associated with the wave convergence fields. The relative roles of these three mechanisms in generating the observed variances in the tropics are still uncertain at the present time.

It is also unclear how much of tropical variances are attributable to Rossby–gravity and Kelvin waves. Despite the fact that Rossby–gravity waves and Kelvin waves are relatively easily identified in the tropical stratosphere, few studies have been able to systematically identify them in the troposphere. Recent numerical studies of the stratospheric QBO suggest that neither the observed Kelvin waves nor the observed Rossby–gravity waves at the tropopause level are strong enough to force the easterly and westerly phases of the QBO oscillation (Takahashi and Boville 1992). It is presumed then that gravity waves also play a strong role in forcing the stratospheric QBO. This leads to the question of how much of the variances in tropical variables are due to gravity waves.

Furthermore, what are the spatial and time variabilities of tropical waves? What factors control their variations? Waves in the tropical stratosphere have been shown to have large geographic, seasonal, and interannual variabilities (Maruyama 1991). Rossby–gravity wave activities revealed by Hendon and Liebmann

*Corresponding author address:* Dr. Minghua Zhang, Institute for Terrestrial and Planetary Atmospheres, State University of New York, Stony Brook, NY 11794-5000.

(1991) in the troposphere are mostly restricted to the central Pacific during the boreal fall season. Maruyama and Tsuneoka (1988) argued that the 1972 El Niño event weakened Rossby–gravity wave activity, leaving the Kelvin waves to force a quickly descending and long-lasting westerly phase of the stratospheric QBO. Yanai and Lu (1983), however, found very different wave activities between the two El Niño events in 1967 and 1972. If these variabilities exist, it is possible that large variations in tropospheric waves could have large influences on the variability of the stratospheric QBO.

It is beyond the scope of the present study to explore all of these questions. In this paper, we present one of the possible mechanisms that could affect the excitation and variability of tropical waves. We study waves that are generated by wave–CISK. This is not only because wave–CISK might be important as a wave generation mechanism, but also due to the belief that most tropical waves are strongly coupled with convective activity. A compromise made in this study is to linearize the problem. As reported in many studies, linear wave–CISK produces the unrealistic result that small-scale disturbances are the most unstable. This drawback can be overcome, under certain circumstances, by using nonlinear positive-only condensational heating or by including some other linear physics in the CISK model (Lau and Peng 1987; Lim et al. 1990; Wang and Rui 1990).

Wave–CISK models generally contain two types of unstable modes (Chang and Lim 1988). One is from static instability that corresponds to a negative effective lapse rate (Gill 1982). The other is a propagating unstable mode that is not related to static instability. It is the latter case that forms the subject of the present study. Past studies of this type of instability have been mostly concerned with Kelvin waves. This is partly due to the similarities between the theoretically modeled unstable modes and the observed 30–50 day oscillations. A focus has been to clarify how the CISK heating slows down wave propagation and makes the period of an unstable mode much longer than that of the neutral free mode and comparable with the observed period. Little attention has so far been paid to the role of the basic flow in the wave–CISK problem. As will be shown, the specific form of the CISK heating and the generation of potential energy in CISK require that the unstable waves tilt backward with height relative to their direction of propagation. Structures of Kelvin waves therefore tilt westward with height, while those of Rossby–gravity waves tilt eastward with height. This is just the opposite of the slopes of these waves that propagate energy upward in the stratosphere. These structures can be greatly affected by the presence of a basic flow with vertical shear. When the vertical shear of the basic flow is in the direction of the vertical tilt of the unstable waves, the basic flow makes the unstable waves tilt further and enhances their instability. In contrast, when the vertical shear of the basic flow is against the vertical tilt of the unstable waves, it suppresses their instability. Kelvin waves and other kinds of eastward propagating waves are more easily excited in a basic flow with westward vertical shear than they are in a flow with eastward vertical shear, while Rossby–gravity waves and other kinds of westward propagating waves are more easily excited in a basic flow with eastward vertical shear.

The paper is organized as follows. Section 2 outlines the model used for the subsequent calculations. Sections 3 and 4 present analyses and discussions for Kelvin and Rossby–gravity waves. Section 5 gives calculations for internal gravity and Rossby waves. The last section is a brief summary.

## 2. The model

A log-pressure vertical coordinate system is used such that $z = -H \ln(p/p_s)$, where $H$ is the scale height, which is taken to be constant, $p = p_s e^{-z/H}$, and $\rho_o = \rho_{os} e^{-z/H}$. The linearized equations for perturbed motion about a zonal flow $\bar{u}(z)$ on an equatorial $\beta$ plane can be written as follows, with the meaning of the symbols as commonly used:

$$\frac{Du}{Dt} - \beta y v + w \frac{\partial \bar{u}}{\partial z} = -\frac{\partial \phi}{\partial x} \tag{1}$$

$$\frac{Dv}{Dt} + \beta y u = -\frac{\partial \phi}{\partial y} \tag{2}$$

$$\frac{D}{Dt}\frac{\partial \phi}{\partial z} - \beta y v \frac{\partial \bar{u}}{\partial z} + N^2 w = \frac{R\dot{Q}}{C_P H} \tag{3}$$

$$\frac{\partial u}{\partial x} + \frac{\partial v}{\partial y} + \frac{\partial(\rho_o w)}{\rho_o \partial z} = 0 \tag{4}$$

$$T = \frac{H}{R}\frac{\partial \phi}{\partial z}, \tag{5}$$

where

$$N^2 = \frac{R}{H}\left(\frac{\partial T_o}{\partial z} + \frac{\kappa T_o}{H}\right)$$

and

$$\frac{D}{Dt} = \frac{\partial}{\partial t} + \bar{u}(z)\frac{\partial}{\partial x}.$$

The total cumulus heating in a vertical column is assumed to be equal to the latent heat carried by convergent moisture below cloud bottom, which is taken to be at $z = z_{cb}$. Thus,

$$\int_0^{z_t} \dot{Q}\rho_o dz = -L\int_0^{z_{cb}} \nabla\cdot(\mathbf{v}q)\rho_o dz, \tag{6}$$

where $z_t$ is the height of the model top. The vertical heating profile is taken to be

$$\dot{Q} = Q_0 \eta(z),$$

where

$$\frac{g}{p_s - p_t}\int_0^{z_t} \eta\rho_o dz = 1 \tag{7}$$

and $p_s$, $p_t$ represent pressures at the surface and tropopause levels. Then,

$$Q_0 = -\frac{gL\int_0^{z_{cb}} \nabla\cdot(\mathbf{v}q)\rho_o dz}{p_s - p_t}. \tag{8}$$

In reality, (6) may not be true because part of the condensed water is detrained out of the clouds and evaporates to the adjacent free atmosphere, therefore producing no net heating. Since no explicit equation for moisture is used here and the physical formulation of heating is not the purpose of this study, we simplify the situation by introducing an efficiency factor $m$ to account for such factors. This heating formulation is a simple analog to Kuo's cumulus parameterization scheme that is used in many general circulation models, with the important exception that negative heating can be present in our simplified formulation, an unrealistic feature but one that facilitates simple mathematical solution.

Our model does not include momentum exchange by cumulus convection, although cumulus momentum mixing might affect wave structures, as was suggested by Stevens et al. (1977). The vertical stability of the basic state is also important in CISK as was shown by Wang (1987); however, it is taken to be fixed in this model. This does not pose any problem because latent heating serves to reduce the basic stability (Gill 1982) and a range of heating profiles is used. Basically, the philosophy of this paper is to employ the simplest model structure that preserves the essential features of the problem.

Rigid boundary conditions are taken at the top and bottom of the model. The upper boundary condition therefore rules out upward propagation of tropospheric waves to the stratosphere. This is not crucial here since the purpose of this study is to examine the excitation of tropospheric waves by convective heating. The absence of a lower boundary layer in the model formulation excludes the presence of Ekman–CISK. Convergent motion, which provides latent heating in this model, is thus purely from the wave dynamics. The two boundary conditions also imply nontilting vertical wave structures if the waves are neutral. Tilt becomes possible only when the waves are unstable.

With the above assumptions, the total energy budget is

$$\frac{\partial}{\partial t}\iiint \frac{1}{2}\left[u^2 + v^2 + \frac{1}{N^2}\left(\frac{\partial\phi}{\partial z}\right)^2\right]\rho_0 dxdydz$$
$$= \iiint\left(-uw\frac{\partial\bar{u}}{\partial z} + v\frac{\partial\phi}{\partial z}\frac{\beta y}{N^2}\frac{\partial\bar{u}}{\partial z} + \frac{R}{N^2C_PH}Q\frac{\partial\phi}{\partial z}\right)\times\rho_0 dxdydz. \tag{9}$$

The necessary condition for CISK is that the last term in the integrand on the right side is positive when integrated over the domain. Thus, heating must be positively correlated with temperature.

For maximum simplification, the troposphere is discretized into three layers as shown in Fig. 1. The discretized equations are

$$\frac{\partial u_i}{\partial t} + \bar{u}_i\frac{\partial u_i}{\partial x} - \beta y v_i + \frac{(w_{i+1} + w_{i-1})}{2}\left(\frac{\partial\bar{u}}{\partial z}\right)_i = -\frac{\partial\phi_i}{\partial x} \tag{10}$$

$$\frac{\partial v_i}{\partial t} + \bar{u}_i\frac{\partial v_i}{\partial x} + \beta y u_i = -\frac{\partial\phi_i}{\partial y} \tag{11}$$

$$\frac{\partial u_i}{\partial x} + \frac{\partial v_i}{\partial y} + \frac{(\rho_o w)_{i+1} - (\rho_o w)_{i-1}}{(\rho_o\Delta z)_i} = 0 \tag{12}$$

for $i = 1, 3, 5$ with $w_0 = w_6 = 0$ and $\Delta z_i = z_{i+1} - z_{i-1}$, and

$$\frac{\partial}{\partial t}\left(\frac{\phi_{i+1} - \phi_{i-1}}{\Delta z_i}\right) + \bar{u}_i\frac{\partial}{\partial x}\left(\frac{\phi_{i+1} - \phi_{i-1}}{\Delta z_i}\right) - \beta y v_i\left(\frac{\partial\bar{u}}{\partial z}\right)_i + N^2 w_i = \frac{RQ_0\eta_i}{C_PH} \tag{13}$$

for $i = 2, 4$. We take the moisture supply to be confined to the lower half-layer of the first model layer, where a constant specific humidity $\bar{q}_{01}$ is specified. With the efficiency coefficient as $m$, (8) is approximated as

$$Q_0 = -\frac{mgL\bar{q}_{01}\bar{\rho}_{o01}(\Delta z)_1}{2(p_s - p_t)}\nabla\cdot\mathbf{v}_1. \tag{14}$$

The zonal basic flow is taken as a linear function of height in this study,

$$\bar{u}(z) = \alpha(z - z_3).$$

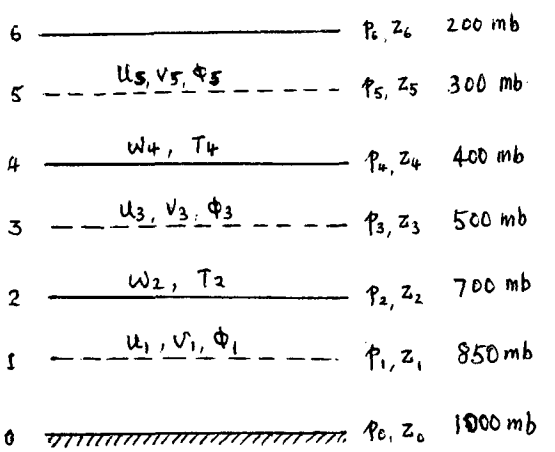


FIG. 1. Model structure.

The range for $\alpha$ that will be explored is $|\alpha| \leq 0.8$ m s$^{-1}$/km. Here $\alpha < 0$ corresponds to a basic flow with westward (or easterly) vertical shear with easterly flow in the upper troposphere and westerly flow in the lower troposphere, while $\alpha > 0$ corresponds to the reverse circulation. The easterly and westerly shear ranges are both within the observational limit of zonal wind variations in the tropics. In fact, Yasunari (1989) showed that the tropospheric zonal wind over Singapore changes from $\alpha > 0$ to $\alpha < 0$ with a near QBO frequency.

The vertical structure of the heating $\eta(z)$ is only represented by the ratio between the total heating in the upper layer to that in the lower layer by $H4/H2 = \Delta p_4\eta_4/\Delta p_2\eta_2$ in this model with coarse vertical resolution. They are further constrained by (7). A range of heating ratios $H4/H2$ and efficiency factors $m$ will be used in our calculations. Values of $m$ larger than 1 are considered to look into the uncertainties of parameters in (14); $\Delta z_i$ is taken as in Fig. 1; $N^2 = 1.35 \times 10^{-4}$ s$^{-2}$, which is equivalent to a lapse rate of about 6.0°C km$^{-1}$. The scale height $H$ is taken as 8 km; $\rho_1$ and $\bar{q}_{01}$ are equal to 1 kg m$^{-3}$ and 10.0 g kg$^{-1}$, respectively.

## 3. Kelvin waves

For Kelvin waves, $v_i = 0$ and

$$\beta y u_i = -\frac{\partial \phi_i}{\partial y}.$$

Let $(u, \phi, w) = (u_k, \phi_k, w_k)e^{ik(x-ct)}$ and omit the wavenumber subscript $k$. Thus, (10), (12), and (13) become

$$ik(\bar{u}_i - c)u_i + \frac{(w_{i+1} + w_{i-1})}{2}\bar{u}_{zi} = -ik\phi_i \quad (15)$$

$$iku_i + \frac{(\rho_o w)_{i+1} - (\rho_o w)_{i-1}}{(\rho_o \Delta z)_i} = 0 \quad (16)$$

$$ik(\bar{u}_{i+1} - c)\left(\frac{\phi_{i+2} - \phi_i}{\Delta z_{i+1}}\right) + N^2 w_i$$

$$_{+1} = \frac{RQ_0\eta_{i+1}}{C_P H} = h^*\eta_{i+1}w_2 \quad (17)$$

with $i = 1, 3, 5$ for (15)–(16) and $i = 1, 3$ for (17), where

$$h^* = m\frac{RgL\bar{q}_{01}\bar{\rho}_{o01}\rho_2}{2C_p H\rho_1(p_s - p_t)}.$$

Eliminating $u_i$ between (15) and (16), one gets

$$-\left[(\bar{u}_i - c)\frac{\rho_{oi+1}}{\rho_{oi}\Delta z_i} - \frac{\bar{u}_{zi}}{2}\right]w_{i+1}$$

$$+\left[(\bar{u}_i - c)\frac{\rho_{oi-1}}{\rho_{oi}\Delta z_i} + \frac{\bar{u}_{zi}}{2}\right]w_{i-1} = -ik\phi_i. \quad (18)$$

After further elimination of $\phi_i$ between (17) and (18), the controlling equations for vertical velocity become

$$A_1(c)w_4 + A_2(c)w_2 = h^*\eta_2 w_2 \quad (19)$$

$$A_3(c)w_4 + A_4(c)w_2 = h^*\eta_4 w_2, \quad (20)$$

where

$$A_1(c) = \frac{(\bar{u}_2 - c)}{\Delta z_2}\left[(\bar{u}_3 - c)\frac{\rho_{o4}}{\rho_{o3}\Delta z_3} - \frac{\bar{u}_{z3}}{2}\right]$$

$$A_2(c) = -\frac{(\bar{u}_2 - c)}{\Delta z_2}\left[(\bar{u}_3 - c)\frac{\rho_{o2}}{\rho_{o3}\Delta z_3} + \frac{\bar{u}_{z3}}{2} + (\bar{u}_1 - c)\frac{\rho_{o2}}{\rho_{o1}\Delta z_1} - \frac{\bar{u}_{z1}}{2}\right] + N^2$$

$$A_3(c) = -\frac{(\bar{u}_4 - c)}{\Delta z_4}\left[(\bar{u}_5 - c)\frac{\rho_{o4}}{\rho_{o5}\Delta z_5} + \frac{\bar{u}_{z5}}{2} + (\bar{u}_3 - c)\frac{\rho_{o4}}{\rho_{o3}\Delta z_3} - \frac{\bar{u}_{z3}}{2}\right] + N^2$$

$$A_4(c) = \frac{(\bar{u}_4 - c)}{\Delta z_4}\left[(\bar{u}_3 - c)\frac{\rho_{o2}}{\rho_{o3}\Delta z_3} + \frac{\bar{u}_{z3}}{2}\right].$$

The propagation speed and growth rate of the waves are obtained by solving the following fourth-order equation:

$$A_1(c)[A_4(c) - h^*\eta_4] - A_3(c)[A_2(c) - h^*\eta_2] = 0. \quad (21)$$

The waves derived here describe Kelvin waves in a basic flow with vertical shear. It is seen that $c$ is independent of the wavenumber $k$, so the Kelvin waves are nondispersive. Thus, as is well known, in linear CISK theory, the shortest waves are the most unstable. This same problem has also been found to occur by Crum and Dunkerton (1992) in some cases when positive-only conditional heating is used. Yet, as discussed in the Introduction, under certain circumstances, this may be overcome by including additional physics in the model (Lau and Peng 1987; Wang and Rui 1990).

We first show calculations with no basic flow in the Kelvin wave–CISK. Figures 2a and 2b give the real and imaginary parts of the phase speed as functions of the heating profile parameter $H4/H2$. The efficiency factor $m$ is taken as 1.0. As has been revealed in many previous studies (e.g., Chang and Lim 1988), when upper-level heating becomes larger than that at lower levels, the two eastward propagating modes coalesce, and the waves are unstable. Figures 2c and 2d show the corresponding $c_r$ and $c_i$ when the heating efficiency factor is increased to $m = 1.5$. It is seen that propagation speed of the two modes decreases. This is because the effective stability ($N^2 - h^*\eta_2$) in (17) is reduced. Furthermore, another branch of instability appears on the left side where $H4/H2$ is small or the lower-level

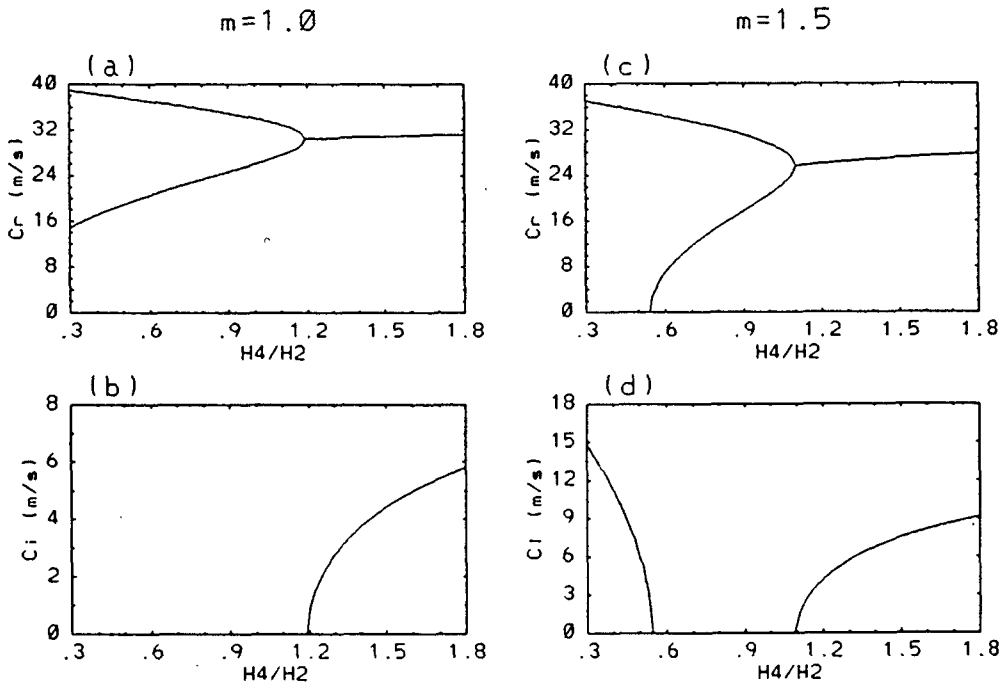


FIG. 2. Real and imaginary parts of the Kelvin wave phase speed as functions of heating profile parameter $H4/H2$ for (a) and (b) $m = 1.0$; (c) and (d) $m = 1.5$.

heating is large (Fig. 2d). This unstable mode is stationary and corresponds to static instability in which the effective stability is negative. Although this is a physical mode, it is not equatorially trapped, as could be deduced from (14) and (15) when $\bar{u} = 0$ and $c$ is purely imaginary. Therefore, it is not considered any further here.

For the case of CISK in a basic flow with vertical shear, Figs. 3a and 3b show the real and imaginary parts of the phase speed as functions of the vertical shear. The efficiency factor $m$ is taken as 1.0 and the heating ratio $H4/H2$ is equal to 1.3. Instability is enhanced when the shear is negative or westward. It is completely suppressed when the shear is sufficiently positive or eastward ($\alpha \geq 0.4$). Calculation of the energy budget shows that growing waves draw energy from the latent heat, and deposit part of it to the basic flow, with the magnitude of the first term on the right-hand side of (9) being about 5% of the last term.

This conclusion is qualitatively unchanged for different heating efficiencies. This is seen in Fig. 4a, where the imaginary phase speed is plotted against $m$ and the shear parameter $\alpha$. Figures 4b and 4c show the corresponding propagation speeds of the two modes. Figure 5 shows $c_i$ as a function of $\alpha$ and the heating profile $H4/H2$ with $m = 1.0$. For the entire parameter range explored here, a basic flow with westward vertical shear enhances Kelvin wave instability, while eastward shear flow suppresses its instability.

This effect of the vertical shear of the basic zonal flow on Kelvin wave–CISK can be explained by examining the vertical structures of the Kelvin wave–CISK modes. For free neutral Kelvin modes in a resting atmosphere with no latent heating, it is seen from (15) and (17) that the pressure field is always in phase with that of the perturbed zonal velocity, while the phase of the temperature field is always 90° ahead of that of the vertical velocity, so that maximum temperature propagates eastward behind the maximum downward vertical velocity. This is shown schematically in Fig. 6a. For an increasing CISK mode, the pressure gradient force should act to accelerate the horizontal flow. This is accomplished by a westward shift in the pressure field at both high and low levels (Fig. 6b). It is not necessary, in general, that this shift be identical at both levels as pictured, however, but only that these shifts be less than 180° to give the required accelerations. Given the CISK mechanism as well as the positive effective stability, that is, $N^2 - h^*\eta_2 > 0$ in (17), upward (downward) motion at low levels implies cold (warm) air at low levels. The westward shift in the pressure field must imply a westward shift in the maximum thickness or mean temperature field, implying that warm (cold) air must exist at high levels overlying the cold (warm) centers at low levels. This implies a westward tilt to the growing waves. Note that this configuration implies both a positive correlation between CISK heat-

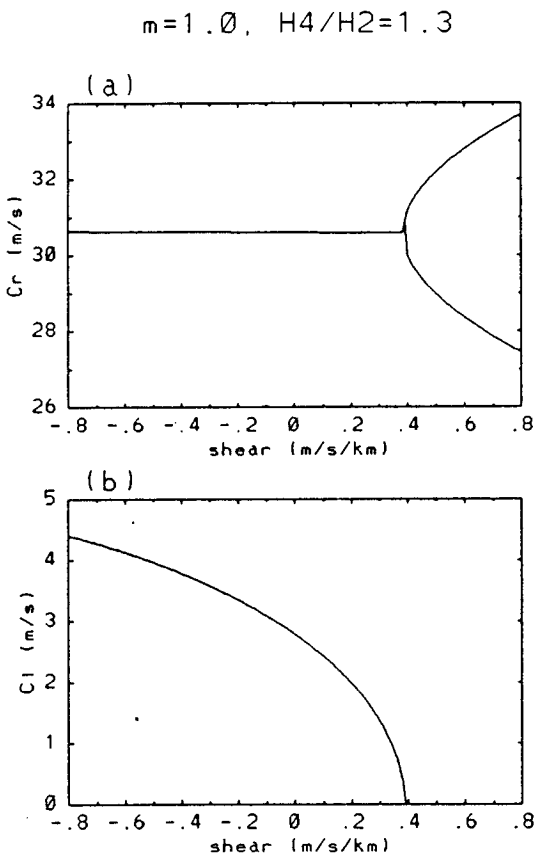


FIG. 3. Phase speeds $c_r$ and $c_i$ of Kelvin waves as functions of the vertical shear of basic flow for $m = 1$ and $H4/H2 = 1.3$.

ing and warm temperature when averaged throughout the troposphere and acceleration of the east–west circulation by horizontal pressure forces leading to a growing wave.

Structures of the Kelvin waves in CISK are shown in Fig. 7a, when $m = 1.0$ and $H4/H2 = 1.3$ are used in a resting atmosphere. It is of interest to note that this structure of the Kelvin wave–CISK mode is opposite to those of Kelvin waves in the stratosphere where upward energy propagation requires an eastward tilt with height. Similar to what is demonstrated in the schematic picture of Fig. 6b, the westward tilt of the wave implies potential energy generation and thus wave growth. The features here are consistent with the Kelvin–CISK calculations of Chang et al. (1988) and numerical simulations of Lau and Peng (1987). They are also seen in the analysis of tropical low-frequency oscillations from general circulation model simulations, which are considered as moist Kelvin modes [Fig. 10 in Lau and Lau (1986), for example].

It is now clear as to why a moderate vertical shear of the basic zonal flow can strongly affect Kelvin wave–CISK. In Fig. 7b, the vertical structure of the unstable Kelvin mode is plotted for our calculation for basic flow with westward vertical shear. Also shown in Fig. 7b is the basic flow used in the calculation. The basic flow in this case provides an environment that makes the wave tilt more strongly than it does for a resting atmosphere. From the energy point of view, the basic flow acts to further align the upper-level maximum temperature toward the low-level upward velocity so that the energy generation becomes larger. This wave is more unstable than in the resting atmosphere case, as is seen from the values of the imaginary phase speed. In contrast, when eastward vertical shear is used, instability disappears, and two neutral modes exist. Their vertical structures are shown in Figs. 7c and 7d. The eastward shear of basic flow eliminates the westward tilt

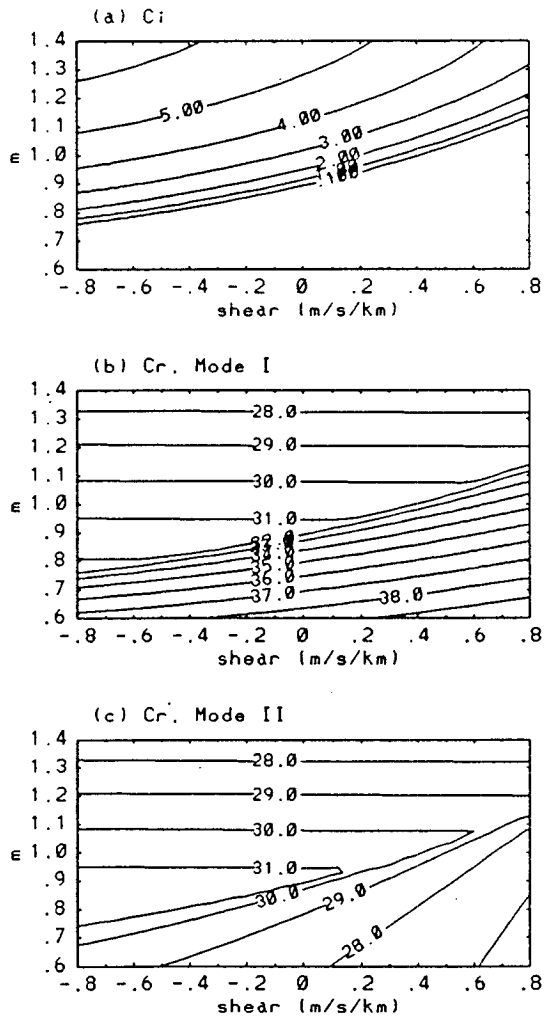


FIG. 4. Phase speed of Kelvin waves as functions of the basic flow shear and heating efficiency factor $m$: (a) $c_i$; (b) and (c) $c_r$ of the two modes. $H4/H2 = 1.3$.

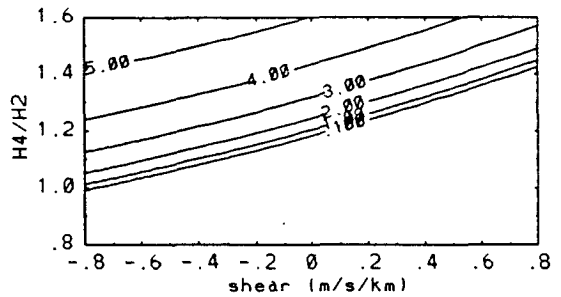


FIG. 5. Phase speed $c_i$ of Kelvin waves as functions of the basic flow shear and heating profile parameter $H4/H2$; $m = 1.0$.

of Kelvin mode in Fig. 7a and renders the waves stable.

## 4. Rossby–gravity waves

For the Rossby–gravity wave case, let

$$(u, v, \phi, w) = (u_k, v_k, \phi_k, w_k) \times \exp\left[ik(x - ct) - \frac{l^2(z)}{2}y^2\right],$$

where $k$ is zonal wavenumber and $l$ is to be determined. Omitting the subscript $k$, Eqs. (1)–(4) become

$$ik(\bar{u} - c)u - \beta yv + w\bar{u}_z = -ik\phi \quad (22)$$

$$ik(\bar{u} - c)v + \beta yu = -\frac{\partial\phi}{\partial y} + l^2y\phi \quad (23)$$

$$ik(\bar{u} - c)\left[\frac{\partial\phi}{\partial z} - y^2l\frac{dl}{dz}\phi\right] - \beta yv\bar{u}_z + N^2w = h^*\eta w_{cb} \quad (24)$$

$$iku + \frac{\partial v}{\partial y} - l^2yv + \frac{\partial w}{\partial z} - y^2l\frac{dl}{dz}w - \frac{w}{H} = 0. \quad (25)$$

Expand $(u, v, \phi, w)$ in the meridional direction by Hermite polynomials $H_0(\zeta) = 1$, $H_1(\zeta) = 2\zeta$, $H_2(\zeta) = 4\zeta^2 - 2$, $\cdots$

$$(u, v, \phi, w) = \sum_{n=0}^{\infty}(u_n, v_n, \phi_n, w_n)H_n(\zeta),$$

where $\zeta = ly$, and make use of the recursion relations

$$\frac{dH_n}{d\zeta} = 2nH_{n-1}$$

$$\zeta H_n = \frac{1}{2}(H_{n+1} + 2nH_{n-1})$$

$$\zeta^2H_n = \frac{1}{4}[H_{n+2} + 2(2n + 1)H_n + 4n(n - 1)H_{n-2}].$$

Equations (22)–(25) are written as

$$ik(\bar{u} - c)u_n - \frac{\beta l^{-1}}{2}[v_{n-1} + 2(n + 1)v_{n+1}] + \bar{u}_zw_n = -ik\phi_n \quad (26)$$

$$ik(\bar{u} - c)v_n + \frac{\beta l^{-1}}{2}[u_{n-1} + 2(n + 1)u_{n+1}] = -2l(n + 1)\phi_{n+1} + \frac{l}{2}[\phi_{n-1} + 2(n + 1)\phi_{n+1}] \quad (27)$$

$$ik(\bar{u} - c)\left[\frac{\partial\phi_n}{\partial z} - l^{-1}\frac{dl}{4dz}(\phi_{n-2} + 2(2n + 1)\phi_n + 4(n + 2)(n + 1)\phi_{n+2})\right] - \frac{\beta}{2l}(v_{n-1} + 2(n + 1)v_{n+1})\bar{u}_z + N^2w_n = h^*\eta w_{cbn} \quad (28)$$

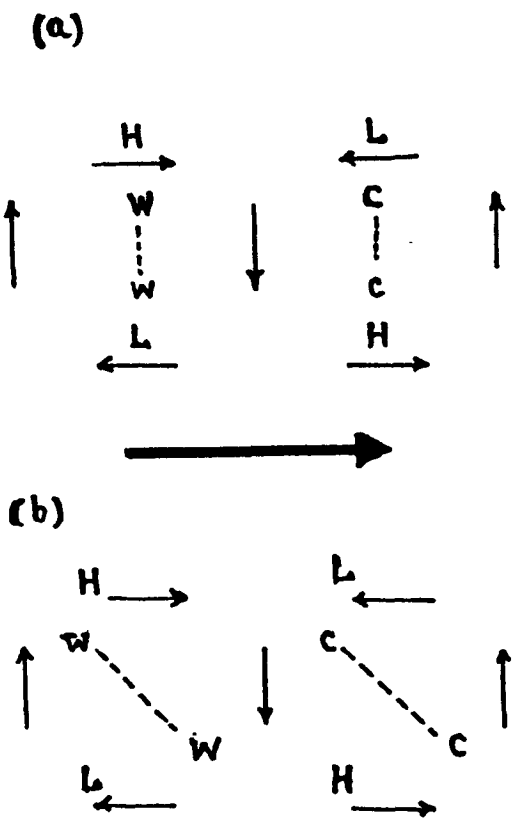


FIG. 6. Schematic view of (a) the eastward-propagating neutral wave and (b) growing wave. Light arrows denote the velocity field. Heavy arrow points to the direction of wave propagation. Symbols w and c represent warm and cold centers; H and L represent high and low centers of the pressure field.

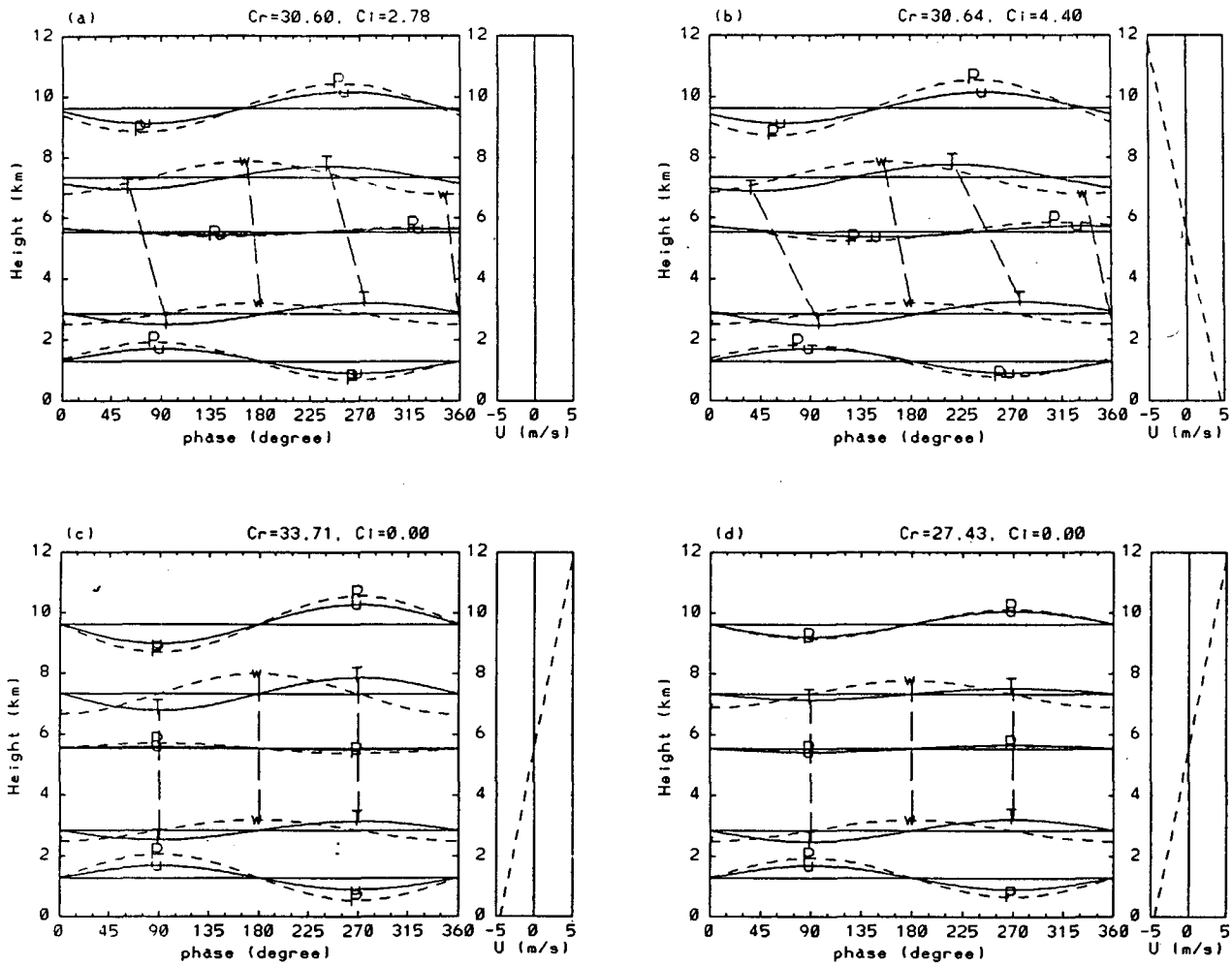


FIG. 7. Vertical structures of Kelvin waves calculated with the basic zonal flow shown as dashed line on the left side of each panel for $m = 1.0$ and $H4/H2 = 1.3$. (a) Rest atmosphere; (b) shear $-0.8$ m s$^{-1}$/km; (c) and (d) neutral modes from shear 0.8 m s$^{-1}$ km$^{-1}$.

$$iku_n + 2l(n+1)v_{n+1} - \frac{l}{2}[v_{n-1} + 2(n+1)v_{n+1}] + \frac{\partial w_n}{\partial z} - l^{-1}\frac{dl}{4dz}[w_{n-2} + 2(2n+1)w_n + 4(n+2)(n+1)w_{n+2}] - \frac{w_n}{H} = 0 \quad (29)$$

for $n = 0, 1, 2, \cdots$.

Unlike the situation for Kelvin waves, Eqs. (22)–(25) are not separable in $y$ and $z$. A solution for Eqs. (26)–(29) can be obtained in terms of an infinite series of Hermite polynomials that would contain the Rossby–gravity wave solution as well as other modes. In the following, we consider a nonrigorous solution to Eqs. (26)–(29) in which we will only be concerned with the Rossby–gravity wave, which is the gravest mode with nonzero $v$, or $v_0$, in a resting atmosphere. Thus, we truncate (26)–(29) with $n = 0$ for $v$ and $n = 1$ for $u$, $w$, and $\phi$.[1] It should be noted that $v_n$ should be truncated one order higher or lower than the rest of the variables to ensure a nonzero solution of the truncated system. Thus, with these approximations, the equations governing the Rossby–gravity wave become

$$ik(\bar{u} - c)u_1 - \frac{\beta l^{-1}}{2}v_0 + \bar{u}_z w_1 = -ik\phi_1 \quad (30)$$

$$ik(\bar{u} - c)v_0 + \beta l^{-1}u_1 = -l\phi_1 \quad (31)$$

[1] This nonrigorous, but plausible, approach is used here to obtain a relatively simple solution for the Rossby–gravity wave case without resorting to a completely numerical solution. It is seen that the main result of this analysis is consistent with the more rigorous solutions for the Kelvin, Rossby, and gravity wave cases that together give the main result of this paper. This is that the presence of a westerly shear enhances the CISK instability of easterly propagating waves while suppressing CISK instability of westerly propagating waves, with the opposite being true for an easterly shear.

$$ik(\bar{u}-c)\left[\frac{\partial\phi_1}{\partial z}-\frac{3}{2}l^{-1}\frac{dl}{dz}\phi_1\right]+\frac{\beta}{2l}v_0\bar{u}_z+N^2w_1=h^*\eta w_{cb1} \quad (32)$$

$$iku_1-\frac{l}{2}v_0+\frac{\partial w_1}{\partial z}-\frac{3}{2}l^{-1}\frac{dl}{dz}w_1-\frac{w_1}{H}=0 \quad (33)$$

$$\beta l^{-1}u_1=l\phi_1. \quad (34)$$

With the omission of the vertical momentum transport term $\bar{u}_z w_1$ in (30), which is small compared with the other terms as can be justified from the final solution, the parameter that describes equatorial trapping is obtained from (30), (31), and (34) as

$$l^2=\frac{\beta}{\bar{u}-c}\left(\frac{\beta}{k^2(\bar{u}-c)}-1\right). \quad (35)$$

Thus,

$$u_1=\frac{l^2}{\beta}\phi_1 \quad (36)$$

$$v_0=\frac{2il\phi_1}{k(\bar{u}-c)}. \quad (37)$$

Using (36) and (37), (33) becomes

$$\frac{ikl^2}{\beta}\left(1-\frac{\beta}{k^2(\bar{u}-c)}\right)\phi_1+\frac{1}{\rho_o}\frac{\partial\rho_o w_1}{\partial z}-\frac{3}{2}l^{-1}\frac{dl}{dz}w_1=0. \quad (38)$$

Omitting the subscripts for the Hermite expansion coefficients, (32) and (38) can be written in difference form as in section 2, giving

$$\frac{ik(\bar{u}_i-c)}{\Delta z_i}[\phi_{i+1}-\phi_{i-1}-g_i(\phi_{i+1}+\phi_{i-1})]+\frac{i\beta\bar{u}_z}{2k(\bar{u}-c)}(\phi_{i+1}+\phi_{i-1})+N^2w_i=h^*\eta_i w_2 \quad (39)$$

at levels $i = 2$, 4, and

$$-\frac{ikl_i^4(\bar{u}-c)}{\beta^2}\phi_i+\frac{\rho_{oi+1}w_{i+1}-\rho_{oi-1}w_{i-1}}{\rho_{oi}\Delta z}-\frac{g_i}{\Delta z_i}(w_{i+1}+w_{i-1})=0 \quad (40)$$

at levels $i = 1$, 3, and 5, where

$$g_i=\left[\frac{3}{4}\left(l^{-1}\frac{dl}{dz}\right)_i+\frac{\beta\bar{u}_z}{2k^2(\bar{u}-c)^2}\right]\Delta z_i.$$

By eliminating $\phi_i$ from (39) and (40), the equations controlling the vertical velocity field are found to be

$$B_1(c)w_4+B_2(c)w_2=h^*\eta_2 w_2 \quad (41)$$

$$B_3(c)w_4+B_4(c)w_2=h^*\eta_4 w_2, \quad (42)$$

where

$$B_1(c)=\frac{\beta^2}{\Delta z_2\Delta z_3}(1-g_2)\left(\frac{\rho_{o4}}{\rho_{o3}}-g_3\right)\frac{(\bar{u}_2-c)}{l_3^4(\bar{u}_3-c)}$$

$$B_2(c)=-\frac{\beta^2(\bar{u}_2-c)}{\Delta z_2}\left[\frac{(1-g_2)\left(\frac{\rho_{o2}}{\rho_{o3}}+g_3\right)}{\Delta z_3}\frac{1}{l_3^4(\bar{u}_3-c)}+\frac{(1+g_2)\left(\frac{\rho_{o2}}{\rho_{o1}}-g_1\right)}{\Delta z_1}\frac{1}{l_1^4(\bar{u}_1-c)}\right]+N^2$$

$$B_3(c)=-\frac{\beta^2(\bar{u}_4-c)}{\Delta z_4}\left[\frac{(1-g_4)\left(\frac{\rho_{o4}}{\rho_{o5}}+g_5\right)}{\Delta z_5}\frac{1}{l_5^4(\bar{u}_5-c)}+\frac{(1+g_4)\left(\frac{\rho_{o4}}{\rho_{o3}}-g_3\right)}{\Delta z_3}\frac{1}{l_3^4(\bar{u}_3-c)}\right]+N^2$$

$$B_4(c)=\frac{\beta^2}{\Delta z_4\Delta z_3}(1+g_4)\left(\frac{\rho_{o2}}{\rho_{o3}}+g_3\right)\frac{(\bar{u}_4-c)}{l_3^4(\bar{u}_3-c)};$$

$l_i$ is determined by (35). The phase speed is obtained by solving the following equation (43) using numerical shooting methods:

$$B_1(c)[B_4(c)-h^*\eta_4]-B_3(c)[B_2(c)-h^*\eta_2]=0. \quad (43)$$

Figures 8a and 8b show the real and imaginary parts of the Rossby–gravity wave phase speed as functions of the heating profile parameter $H4/H2$ in an atmosphere with no basic zonal flow. The heating efficiency factor $m$ is again taken as 1.0 and the zonal wavenumber $k$ is taken as 4. Similar to Kelvin wave–CISK, coalescence of the two westward propagating Rossby–gravity waves results in CISK instability when the heating is larger at upper levels. Figures 8c and 8d show

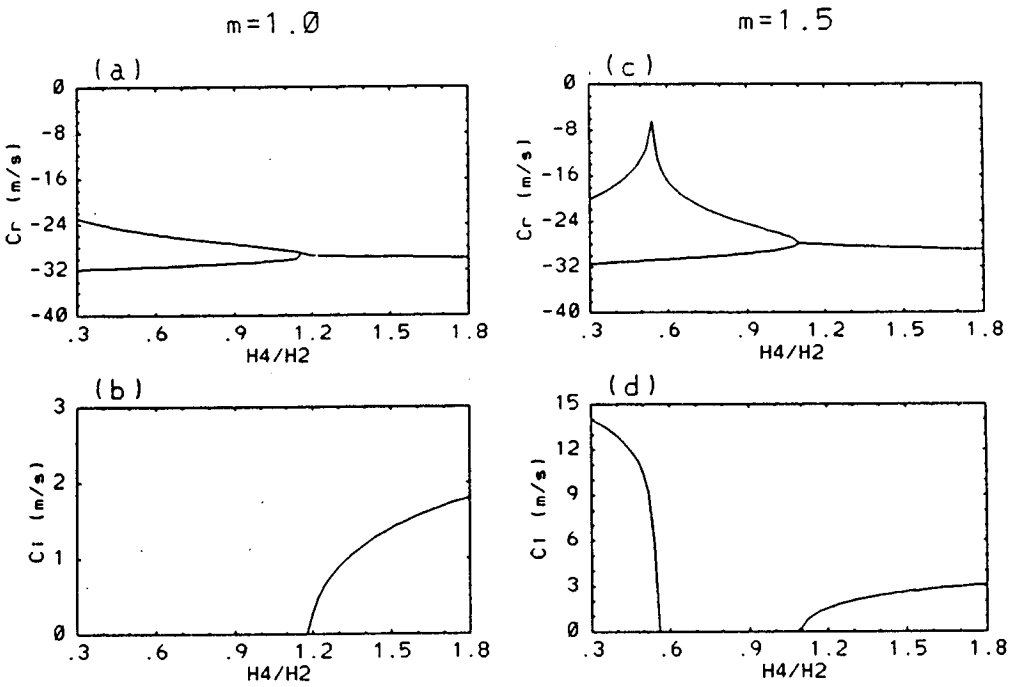


FIG. 8. Real and imaginary parts of the Rossby–gravity wave phase speed as functions of the heating profile parameter $H4/H2$. Zonal wavenumber is 4. (a) and (b) $m$ = 1.0; (c) and (d) $m$ = 1.5.

slower westward propagation speed and one more branch of instability as the heating efficiency factor is increased to $m = 1.5$. The additional unstable mode is the same as was seen in the Kelvin wave case in the sense that it arises from the static instability associated with a negative effective lapse rate. It is different from the Kelvin mode in the sense that it is not stationary. This static instability mode also propagates westward. The criterion of the static instability here is the same as that in the Kelvin wave case; that is, $H4/H2 < 0.56$. This is expected given the cause of the instability. In this particular calculation, the criterion for the other type of instability is also the same as that in the previous section; that is, $H4/H2 > 1.1$. This is not necessarily true in all cases. The amplitude of the statically unstable Rossby–gravity mode amplifies toward higher latitudes. It is therefore not equatorially trapped and will not be discussed further in the following calculations.

For the no-static instability mode, the basic shear zonal flow once again is of significance. Figure 9 presents the real and imaginary parts of the phase speed of the zonal wavenumber 4 Rossby–gravity wave as a function of the vertical shear of the basic flow with all the other parameters having the same value as in Fig. 3. It is seen that the effect of the basic flow vertical shear on Rossby–gravity wave CISK is exactly the opposite of what was seen for the Kelvin wave–CISK, that is to say, eastward vertical shear tends to enhance instability, while westward shear acts to suppress instability. Similar to Kelvin waves, this type of instability derives energy primarily from the last term in (9), that is, the latent heat. Its magnitude is about 20 times as large as the other terms in (9).

This selective role of the vertical shear of the basic flow for Rossby–gravity wave–CISK is shown to be valid also for different heating efficiencies in Fig. 10, where the imaginary and real parts of the phase speed are plotted as functions of $m$ and the shear parameter $\alpha$. It also remains true for different heating profiles, as is shown in Fig. 11, where the heating efficiency factor $m$ is taken to be 1.0. Differences between the effects of basic flow vertical shear on Rossby–gravity waves and Kelvin waves are easily seen when one compares Fig. 10 with Fig. 4, and Fig. 11 with Fig. 5. It is also noted that Rossby–gravity wave–CISK is even more sensitive to the vertical shear of the basic flow than was the case for Kelvin waves.

The vertical structure of the unstable Rossby–gravity wave in a resting atmosphere is shown in Fig. 12a. In the Southern Hemisphere, the sign of the $v$ component needs to be reversed because its Hermite expansion order differs from the rest of the variables in (30)–(34). Since the wave propagates westward, in contrast to the Kelvin wave case that was shown in Fig. 6, the temperature maximum occurs to the east of the maximum downward motion. Wave growth means that the temperature maximum at the lower level is located less than 90° east of the maximum downward motion so that net compressional heating occurs at the warm cen-

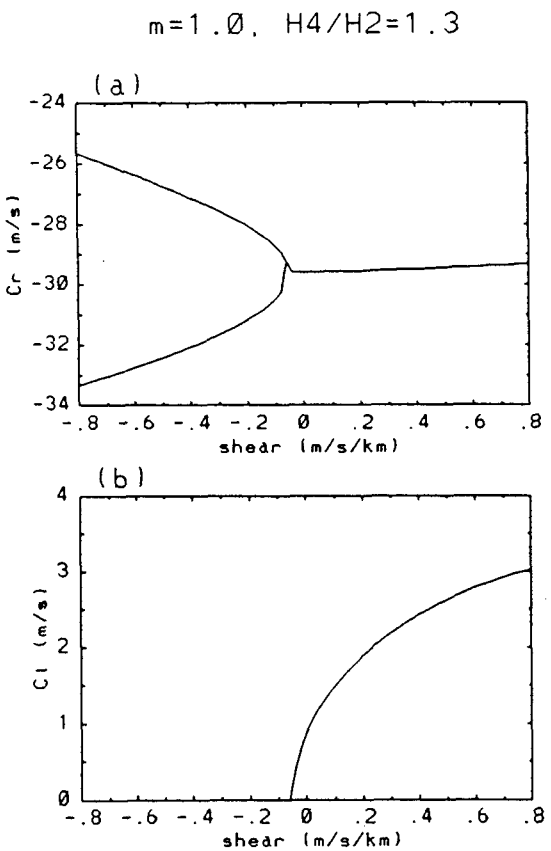


FIG. 9. Phase speed $c_r$ and $c_i$ of Rossby–gravity waves as functions of the vertical shear of basic flow for $m = 1$, $H4/H2 = 1.3$, and $k = 4$.

ter. Maximum temperature thus tilts eastward with increasing height, toward the phase of maximum low-level upward velocity, so that correlation between the temperature and heating is positive and total energy is generated by the latent heating. Therefore, the unstable wave tilts eastward with height. Once again, this is the opposite to the situation for Kelvin wave–CISK. It is also opposite to Rossby–gravity waves in the stratosphere, where their structures tilt westward. This opposite tilting of Rossby–gravity waves in the troposphere and stratosphere is in fact revealed in the observational studies of Hendon and Liebmann (1991, Fig. 9), who found eastward tilt of Rossby–gravity waves below 200 mb.

The effect of the zonal flow vertical shear acts to either further tilt the Rossby–gravity wave or lessen its tilt. Figure 12b is the case when the basic flow (westerly shear) favors greater tilt and thus larger instability. Figures 12c and 12d show the two neutral modes where the shear of the basic flow has eliminated the tilt of the waves so that no energy source can be maintained for wave growth.

The above discussions are for Rossby–gravity waves with zonal wavenumber 4. For other zonal wavenumbers, the growth rates of the unstable modes are shown in Fig. 13, where $m = 1.0$ and $H4/H2 = 1.3$ are still used. It is seen that the discussed role of the basic flow in affecting CISK instability operates for all wavenumbers; that is, eastward vertical shear of the basic flow promotes instability while westward shear diminishes instability. For zonal wavenumbers $k \geq 8$, the effect of the shear is no longer monotonic. This is due to the fact that when the horizontal scale of the Rossby–gravity wave is sufficiently small, the vertical tilt of the wave, enhanced by the advection of the shear basic flow as in Fig. 12b, could displace the upper-level maximum temperature to the east of the low-level upward motion. Therefore, the correlation between the temperature field and the lower-level vertical velocity, which is equivalent to the rate of energy generation, could be reduced and no longer monotonically increases with the increasing shear of the basic flow. In

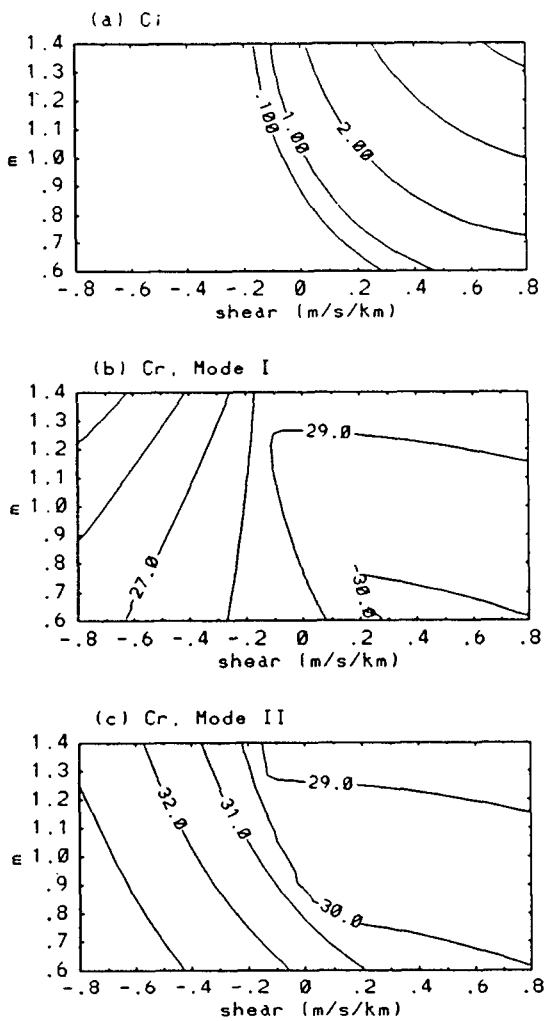


FIG. 10. Phase speed of Rossby–gravity waves as functions of the basic flow shear and heating efficiency factor $m$: (a) $c_i$; (b) and (c) $c_r$ of the two modes. $H4/H2 = 1.3$ and $k = 4$.

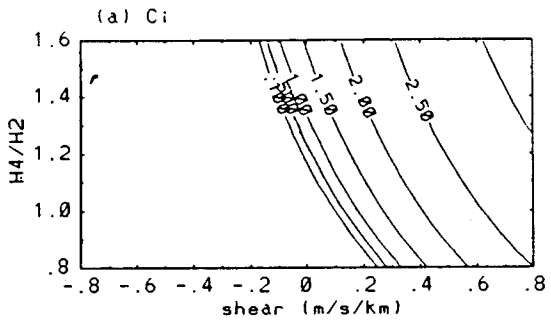


FIG. 11. Phase speed $c_i$ of Rossby–gravity waves as functions of the basic flow shear and heating profile parameter $H4/H2$ for $m = 1.0$ and $k = 4$.

regarding to the most unstable wavenumbers, we see that when the shear is weak, the longest waves are the most unstable. When the shear is large, zonal wavenumbers 4 to 3 are the most unstable. While this cannot simply be claimed as the reason why Rossby–gravity waves with zonal wavenumber 3 to 4 are mostly observed in the stratosphere, the calculations do show that Rossby–gravity wave–CISK can be affected dramatically by the presence of the basic zonal flow.

## 5. Other types of waves

### a. *Internal gravity waves*

It is anticipated that the above mechanism also applies to other types of waves, since the form of the CISK heating and the energy generation requirements are the same. For gravity waves, we can simply set $\beta = 0$ in (1)–(3). By using $(u, v, \phi, w) = (u_{k,l}, v_{k,l}, \phi_{k,l}, w_{k,l})e^{i(kx+ly-kct)}$ and substituting in the equations, one gets the following gravity wave equation for the vertical velocity:

$$(\bar{u} - c)\frac{\partial}{\partial z}\left[(\bar{u} - c)\left(\frac{\partial \rho_o w}{\rho_o \partial z} - \frac{1}{\bar{u} - c}\frac{\partial \bar{u}}{\partial z}w\right)\right] + N^2\frac{k^2 + l^2}{k^2}w = h^*\frac{k^2 + l^2}{k^2}\eta w_{cb}. \quad (44)$$

This equation is approximated by the difference scheme of section 2. The propagation speed and growth rate can be solved for as was done in the previous two sections. In the following calculations, for simplicity, we assume $k = l$; that is, the meridional and longitudinal scales of the gravity wave are the same.

Because of the symmetry of the problem, gravity waves propagate both eastward and westward. In a resting atmosphere, the eastward and westward propagating waves have the same propagation speed and the same growth rate for gravity wave–CISK. However, when a basic flow with vertical shear is present, the waves that propagate in the two directions are affected differently. Figure 14 shows the imaginary phase speed for the eastward propagating wave (solid) and that for the westward propagating wave (dashed) as functions of the vertical shear of the zonal basic flow. In this calculation, the heating efficiency factor $m$ is taken as 1.0 and the heating ratio $H4/H2$ is taken as 1.0. It is seen that eastward vertical shear of the basic flow weakens the instability of the eastward propagating wave but enhances the instability of the westward propagating wave, while the westward vertical shear of the basic flow has the opposite influence.

Figure 15 shows the real and imaginary parts of the phase speed of internal gravity waves in a basic flow with an eastward vertical shear of 0.8 m s$^{-1}$ km$^{-1}$. They are plotted against the heating profile parameter $H4/H2$ and the heating efficiency $m$. As was in the case for Kelvin and Rossby–gravity waves, the larger the heating efficiency factor, the stronger the CISK (Fig. 15c), and the larger the ratio of the upper-layer heating to the lower-layer heating, the stronger the CISK. It is shown in Fig. 15c that the westward propagating wave has a larger unstable domain of heating parameters than does the eastward propagating wave. The westward propagating wave is also more unstable. It is straightforward to show that when this calculation is performed in a basic flow with a westward vertical shear of $-0.8$ m s$^{-1}$ km, the reverse results are seen.

### b. *Rossby waves*

When $\beta y$ is replaced by the Coriolis parameter $f_o = 2\Omega \sin\theta_o$ and the quasigeostrophic approximation is used in (1)–(3), the controlling equation for Rossby wave–CISK is found to be

$$\left[(\bar{u} - c)\frac{\partial}{\partial z} - \frac{\partial \bar{u}}{\partial z}\right]\left[\frac{f_o^2}{\beta - (\bar{u} - c)K^2}\frac{\partial \rho_o w}{\rho_o \partial z}\right] + N^2 w = h^*\eta w_{cb}, \quad (45)$$

where $K^2 = k^2 + l^2$. Once again, the difference form of this equation is used to calculate the real and imaginary parts of the phase speed. Consistent with the quasigeostrophic approximation, we choose $\theta = 30°$N as our reference latitude.

Figure 16 gives the growth rate ($Kc_i$) of the Rossby waves as a function of the basic flow vertical shear for different wavenumbers $K$. The heating parameters $m$ and $H4/H2$ are taken to be 1.0 and 1.3, respectively. Since Rossby waves propagate westward, consistent with the foregoing discussions, eastward vertical shear of the basic flow tends to enhance Rossby wave instability, while westward shear of the basic flow suppresses Rossby wave–CISK. The physical basis for this selective role of the vertical shear is the same as was the case for Rossby–gravity waves. That is, the eastward tilt of Rossby waves in CISK is enhanced by the eastward vertical shear of the basic flow, making

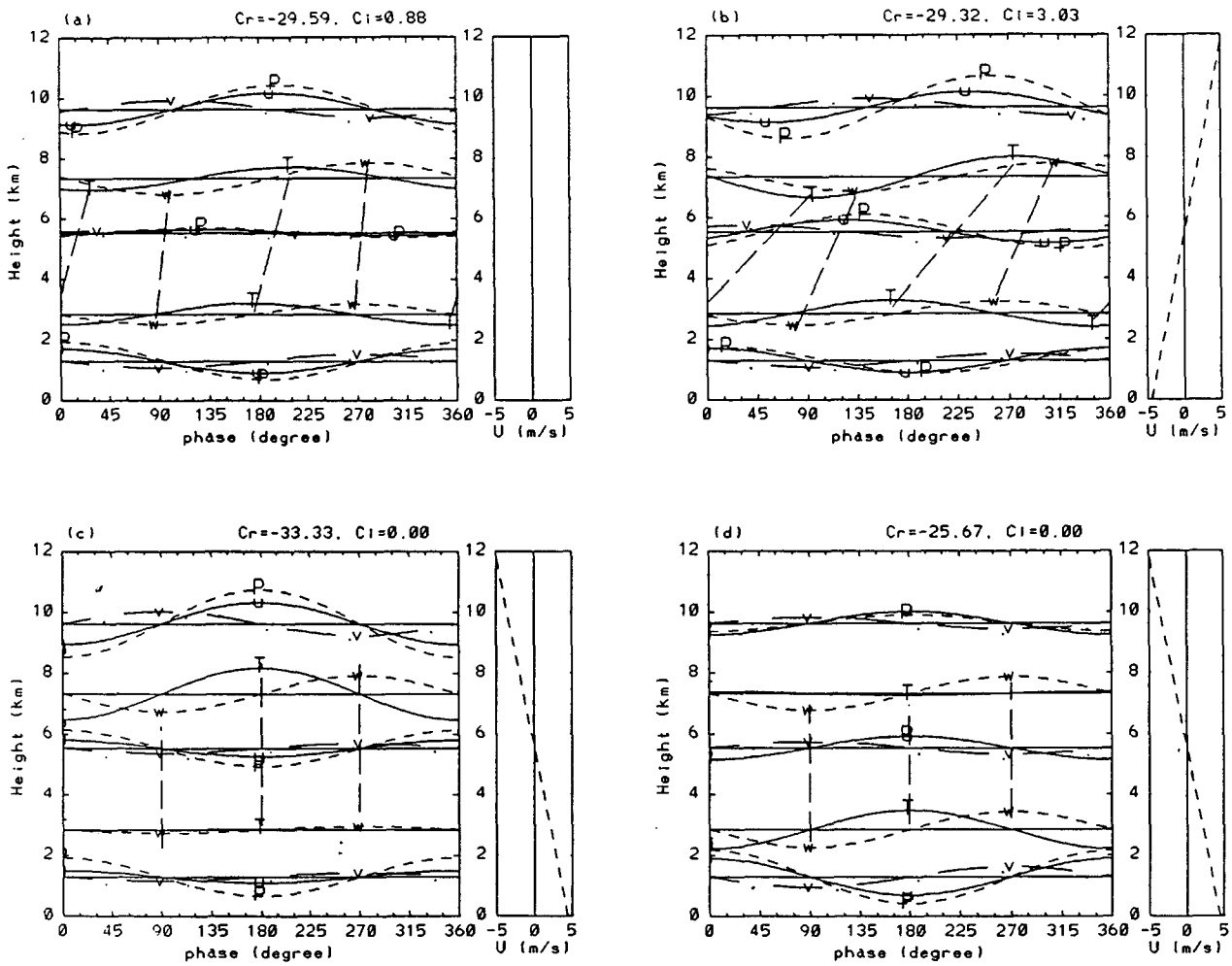


FIG. 12. Vertical structures of Rossby–gravity waves calculated with the basic zonal flow shown as dashed line on the left side of each panel: $m = 1.0$, $H4/H2 = 1.3$, and $k = 4$. (a) Rest atmosphere; (b) shear 0.8 m s$^{-1}$/km; (c) and (d) neutral modes from shear −0.8 m s$^{-1}$/km.

the waves more unstable, while the eastward tilt is diminished by the westward vertical shear of the basic flow, suppressing the energy generation and instability.

## 6. Summary and discussion

Bolton (1980) has extended the Miles theorem (Miles 1961) to wave–CISK models, concluding that the necessary condition for the existence of propagating CISK modes is that the heating is out of phase with the vertical velocity. In most wave–CISK models, heating throughout the troposphere is parameterized by the low-level vertical velocity. Thus, Bolton's extension requires that the upper-level vertical velocity is out of phase with the low-level vertical velocity. A tilt of phase with height therefore becomes inevitable.

The present study has analyzed the vertical structure of wave–CISK through the propagation and energy growth requirements of the unstable modes. It is then shown that this vertical structure is associated with the intensity of CISK and can be greatly affected by a basic flow with vertical shear. When the unstable mode is not from static instability, the effective lapse rate is positive. Propagation of the wave means that the phase of the temperature is ahead of that of the vertical velocity, so that the temperature maximum propagates following the downward motion. Meanwhile, at the level where the vertical velocity is used to parameterize the heating, wave growth requires that the phase difference between temperature and vertical velocity is larger than 90°, so that the warm center is under the descending motion to ensure further growth of the temperature. Looking at this in another way, temperature has to correlate positively with the heating field when integrated over the whole domain so that the total energy of the wave is growing. This means that the temperature field at upper levels is less than 90° ahead of the heating, or less than 90° ahead of the lower-level upward vertical velocity.

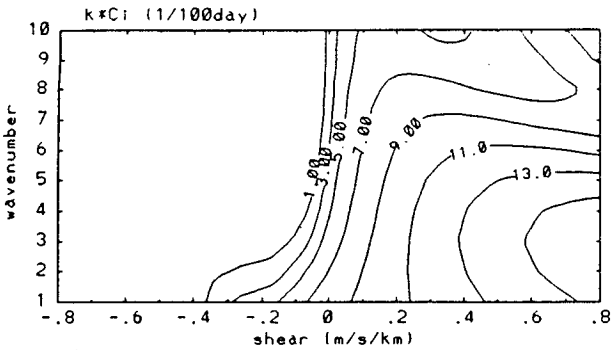


FIG. 13. Growth rate of Rossby–gravity waves as functions of the basic flow shear and zonal wavenumber for $m = 1.0$ and $H4/H2 = 1.3$.

The structure of increasing modes must therefore tilt backward with height with respect to the direction of wave propagation.

The presence of basic flow shear serves to change the tilt of waves. When the basic flow shear is in the direction of wave propagation, its advection acts to counteract the backward tilt of the unstable mode, and so to suppress energy generation and the resulting instability. When the basic flow shear is opposite to the direction of wave propagation, it causes a greater tilt of the wave, enhances the energy production and the resulting instability.

The mechanisms for the formation of the vertical structures of unstable modes and the influence of the basic flow presented above are generally applicable to wave–CISK generation, although no attempt is made in this study to answer what types of waves are more likely to be excited in comparison with the others. These include Kelvin waves, Rossby–gravity waves, gravity waves, and Rossby waves. Eastward propagating waves generated in CISK tilt westward with height. They are more easily excited in a basic flow with westward vertical shear while they are less easily excited in a basic flow with eastward shear. Westward propagating waves arising from CISK tilt eastward with height. They are favored by a basic flow with eastward vertical shear and are suppressed by a basic flow with westward shear.

Lim and Chang (1986) have shown that tropical internal heating can excite only internal waves, while it is the vertical shear of the basic flow that mainly facilitates transfer of energy from internal modes to external modes, which then generate a barotropic-type response and teleconnection pattern in midlatitudes. Their study used a prescribed tropical heating field. The current study shows that the vertical shear of the basic flow is also important for the generation of internal waves.

It is of interest to know to what degree the presented mechanisms operate in the real atmosphere. Because the basic flow can be defined as a long time scale flow with respect to the wave period, it can be subject to large seasonal and interannual variations. It is suggested that tropical waves have large variabilities due to the effects cited here. Certain relationships are then expected between tropical waves and persistent wind systems as well as sea surface temperature distributions. For example, a typical circulation pattern is that vertical wind shear changes signs on two sides over a warm pool of SST, giving the Walker circulation. Such a wind system can facilitate different wave excitations on the two sides of the warm center.

Some cautions should be made in interpreting observations in light of the results obtained here. The main restriction is from the linearized nature of the analysis. Linear studies have provided important insight into our understanding of tropical disturbances. Nevertheless, several studies have shown recently that nonnegative nonlinear heating can greatly alter the CISK behavior from that derived using linear heating (Lim et al. 1990; Crum and Dunkerton 1992). Related discussions about the applicability of linear CISK are found in Wang (1987). Another problem is the formulation of heating. Without a water budget equation and cumulus as well as boundary-layer parameterizations, it is difficult to get realistic heating rates in the CISK problem. Even a different highly parameterized heating, such as the phase-lagged type of CISK heating suggested by Davies (1979), could change the present results, but we believe such differences will be of a quantitative nature rather than being qualitatively different from that derived in the present study. Numerical experiments are currently being planned by the authors to examine the validity of the findings of this study when convection, water vapor, and boundary physics are explicitly included in a nonlinear model. We also plan to relax the rigid upper boundary condition employed in this study to an open boundary, which per-

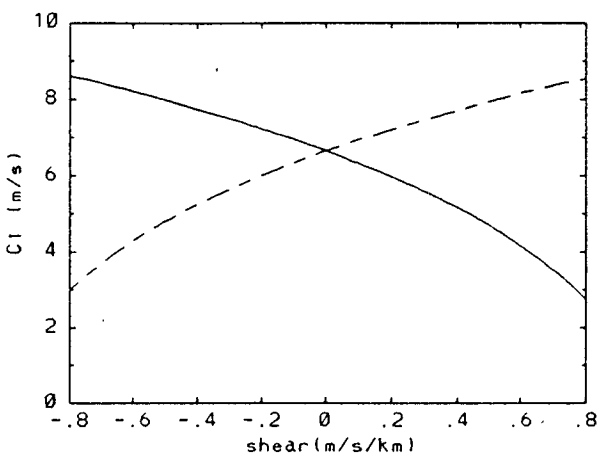


FIG. 14. Phase speed $c_i$ of the eastward propagating gravity wave (solid) and westward propagating gravity wave (dashed) as functions of the basic flow shear. $H4/H2 = 1.0$, $m = 1.0$; $k = l$ is assumed.

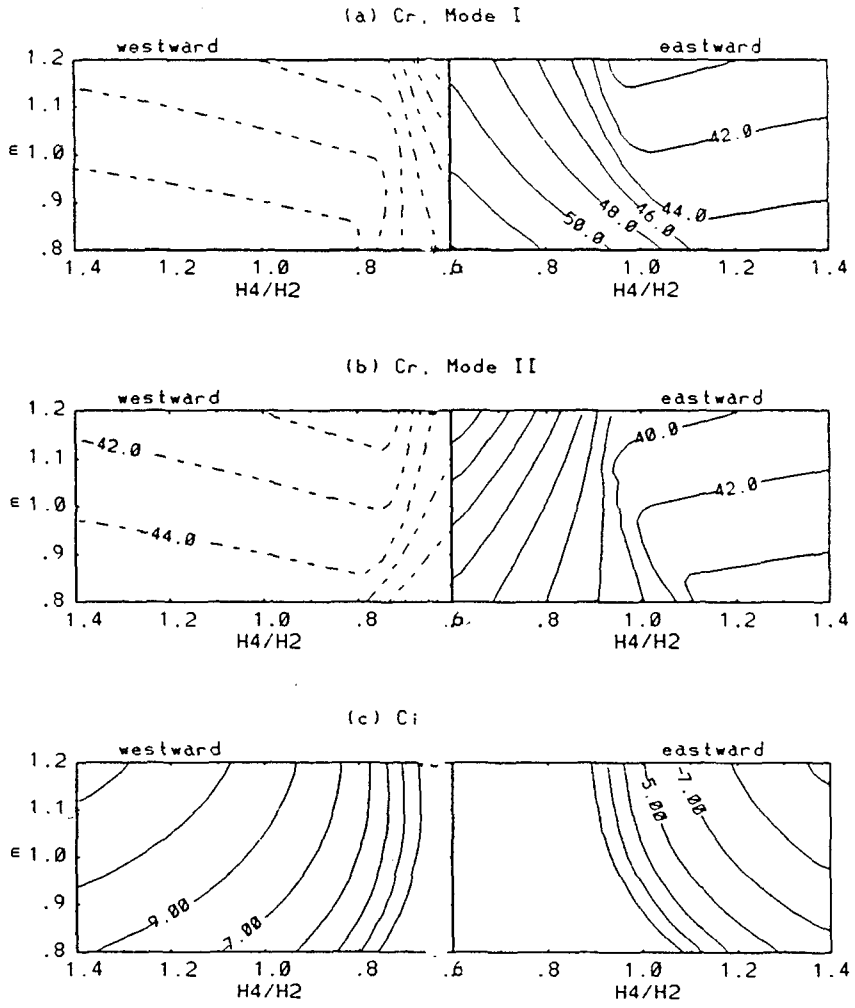


FIG. 15. Phase speed $c_r$ and $c_i$ of the gravity waves in a basic flow with eastward vertical shear of 0.8 m s$^{-1}$/km as functions of heating parameters $H4/H2$ and $m$.

mits propagation of energy from the troposphere to the stratosphere. It is interesting to see how the shear of the zonal flow in the troposphere might be related to the vertical momentum transport into the stratosphere by the tropical waves having their source in the troposphere, and thus with the variability of the stratospheric quasi-biennial oscillation.

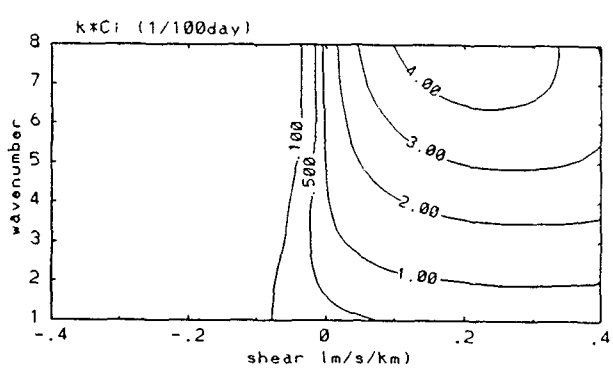


FIG. 16. Growth rate of Rossby waves as functions of the basic flow shear and wavenumber $K$: $m$ = 1.0 and $H4/H2$ = 1.3.

*Acknowledgments.* M. Zhang's participation in this research was supported in part by the DOE Atmospheric and Climate Research Division under Grant DEFG0285-ER60314, and M. Geller's participation was supported in part by NASA Contracts NAG51699, for research relating to the Tropical Rain Measurement Mission, and NAS531720, for interdisciplinary studies of hydrological processes and climate relating to the Earth Observation System. We thank the anonymous reviewers whose comments have led to clarification of the original manuscript.

## REFERENCES

Bolton, D., 1980: Application of the Miles theorem to forced linear perturbations. *J. Atmos. Sci.*, **37**, 1639–1642.

Chang, C. P., and H. Lim, 1988: Kelvin-wave CISK: A possible mechanism for the 30–50 day oscillations. *J. Atmos. Sci.,* **44,** 1709–1720.

Crum, F. X., and T. J. Dunkerton, 1992: Analytic and numerical models of wave–CISK with conditional heating. *J. Atmos. Sci.,* **49,** 1693–1708.

Davies, H. C., 1979: Phase-lagged wave–CISK. *Quart. J. Roy. Meteor. Soc.,* **105,** 325–353.

Gill, A. E., 1982: Studies of moisture effects in simple atmospheric models: the stable case. *Geophys. Astrophys. Fluid Dyn.,* **19,** 119–152.

Hayashi, Y., and D. G. Golder, 1978: The generation of equatorial planetary waves: Control experiments with a GFDL general circulation model. *J. Atmos. Sci.,* **35,** 2068–2082.

Hendon, H. H., and B. Liebmann, 1991: The structure and annual variation of antisymmetric fluctuations of tropical convection and their association with Rossby–gravity waves. *J. Atmos. Sci.,* **48,** 2127–2140.

Holton, J. R., 1972: Waves in the equatorial stratosphere generated by tropospheric heat sources. *J. Atmos. Sci.,* **29,** 368–375.

Itoh, H., and M. Ghil, 1988: The generation mechansim of mixed Rossby–gravity waves in the equatorial troposphere. *J. Atmos. Sci.,* **45,** 585–604.

Lau, K. M., and L. Peng, 1987: Origin of low-frequency (intraseasonal) oscillations in the tropical atmosphere. Part I: Basic theory. *J. Atmos. Sci.,* **44,** 950–972.

Lau, N. C., and K. M. Lau, 1986: The structure and propagation of intraseasonal oscillations appearing in a GFDL general circulation model. *J. Atmos. Sci.,* **43,** 2023–2047.

Lim, H., and C. P. Chang, 1986: Generation of internal- and external-mode motions from internal heating: Effects of vertical shear and damping. *J. Atmos. Sci.,* **43,** 948–957.

——, T. K. Lim, and C. P. Chang, 1990: Reexamination of wave–CISK theory: existence and properties of nonlinear wave–CISK modes. *J. Atmos. Sci.,* **47,** 3078–3091.

Madden, R. A., and P. R. Julian, 1972: Description of global-scale circulation cells in the tropics with a 40–50 day period. *J. Atmos. Sci.,* **29,** 1109–1123.

Mak, M. K., 1969: Lateral driven stochastic motions in the tropics. *J. Atmos. Sci.,* **26,** 41–64.

Maruyama, T., 1991: Annual and QBO-synchronized variations of lower-stratospheric equatorial wave activity over Singapore during 1961–1989. *J. Meteor. Soc. Japan,* **69,** 219–231.

——, and Y. Tsuneoka, 1988: Anomalously short duration of easterly wind phase of the QBO at 50 hPa in 1987 and its relationship to an El Niño event. *J. Meteor. Soc. Japan,* **66,** 629–633.

Matsuno, T., 1966: Quasi-geostrophic motions in the equatorial area. *J. Meteor. Soc. Japan,* **44,** 25–43.

Miles, J. W., 1961: On the stability of heterogeneous shear flows. *J. Fluid Mech.,* **10,** 496–508.

Salby, M. L., and R. R. Garcia, 1987: Transient response to localized episodic heating in the tropics. Part I: Excitation and short-time near-field behavior. *J. Atmos. Sci.,* **44,** 458–498.

Stevens, D. E., R. S. Lindzen, and L. J. Shapiro, 1977: A new model of tropical waves incorporating momentum mixing by cumulus convections. *Dyn. Atmos. Oceans.,* **1,** 365–425.

Swinbank, R., T. N. Palmer, and M. K. Davey, 1988: Numerical simulation of the Madden and Julian oscillation. *J. Atmos. Sci.,* **45,** 774–788.

Takahashi, M., and B. A. Boville, 1992: A three-dimensional simulation of the equatorial quasi-biennial oscillation. *J. Atmos. Sci.,* **49,** 1020–1035.

Wallace, J. M., 1973: General circulation of the tropical lower stratosphere. *Rev. Geophys. Space Phys.,* **11,** 191–222.

——, and V. E. Kousky, 1968: Observational evidence of Kelvin waves in the tropical stratosphere. *J. Atmos. Sci.,* **25,** 280–292.

Wang, B., 1987: The nature of CISK in a generalized continuous model. *J. Atmos. Sci.,* **44,** 1411–1426.

——, and H. L. Rui, 1990: Dynamics of the coupled moist Kelvin–Rossby wave on an equatorial $\beta$ plane. *J. Atmos. Sci.,* **47,** 397–413.

Yanai, M., and T. Maruyama, 1966: Stratospheric wave disturbances propagating over the equatorial Pacific. *J. Meteor. Soc. Japan,* **44,** 291–294.

——, and M. M. Lu, 1983: Equatorial trapped waves at the 200 mb level and their association with meridional convergence of wave energy flux. *J. Atmos. Sci.,* **40,** 2785–2803.

Yasunari, T., 1989: A possible link of the QBOs between the stratosphere, troposphere and sea surface temperature in the tropics. *J. Meteor. Soc. Japan,* **67,** 483–493.

Zangvil, A., and M. Yanai, 1980: Upper tropospheric waves in the tropics. Part I: Dynamical analysis in the wavenumber-frequency domain. *J. Atmos. Sci.,* **37,** 285–298.